

SPECSweb Post-Tracking Classification Method

Doug Grimmett

SPAWAR Systems Center Pacific (SSC-Pac)
San Diego, CA, 92152-5001, U.S.A.
grimmett@spawar.navy.mil

Cherry Wakayama

SPAWAR Systems Center Pacific (SSC-Pac)
San Diego, CA, 92152-5001, U.S.A.
cherry.wakayama@navy.mil

Abstract - The Specular-Cued Surveillance Web (SPECSweb) multistatic tracker effectively reduces false track rate through the use of two amplitude thresholds. A high threshold is used to identify the occurrence of high-strength specular detection cues for track initiation. A low threshold is used for selective extraction of additional detections for track extension forward and backward in time. This approach significantly reduces the node-to-fusion-center communication loading requirements as well as reducing the output false track rate. At the time of the specular-cued track initiation, a historical (back)-track is reconstructed and output. In some cases, there may still be false tracks at the tracker output. We demonstrate a post-tracking classification method which identifies and removes any residual false tracks. Classification feature information for track-associated contacts is passed through the tracker and is available at its output. Discriminating true target tracks from false ones at the tracker output is made using a sequential probability ratio test (SPRT) based on feature information and kinematic track-quality. The method is shown to be effective in reducing false tracks when applied to a simulated data set.

Keywords: Multistatic Sonar – Classification – Multi-Sensor Fusion – Tracking – Cueing – Clutter

1 Introduction

A concept referred to as the “Specular-Cued Surveillance Web (SPECSweb)” is being pursued to mitigate the data-rate overloading problem inherent in multistatic sonar systems. The SPECSweb multistatic tracker does this through an implementation of high and low amplitude thresholds. The high threshold is used to identify the occurrence of high-strength specular detection cues for track initiation. The low threshold is used for a selective, proximity-based extraction of additional detections for track extension backward (from the time of the specular cue) in time. This historical track data is then extended forward in time as new data arrives. This approach provides a robust, automated ASW detection and tracking method, resulting in a significant reduction in false track rates and communication link loading compared to conventional multistatic fusion methods. Although SPECSweb has already been shown to be quite

effective at reducing false tracks [1-3], the work discussed in this paper shows that yet additional reductions are possible through a post-tracking classification method.

There are a number of approaches one may take to perform target classification together with sensor fusion and target tracking, as depicted in figure 1. The traditional approach has been to perform classification prior to the fusion/tracking processes. In this case, firm (accept/reject) decisions for detection contacts are made prior to tracking. This acts as a filter on the data being sent to the fusion algorithm. It is usually performed on individual contacts from a single (source-receiver-waveform) “scan”, and classifies each of them based on statistical properties or physical “features” extracted from the data during upstream signal and information processing. The potential disadvantage of this approach is that the classification process may not be accurate enough or robust, resulting in unacceptable risk of true target dismissal. In this approach, the success of tracking will be largely dependent on the effectiveness of the classification step, since it determines which of the data are made available to the tracking algorithm.

An alternative approach is to integrate the classification process directly into the tracking algorithm itself (sometimes referred to as “feature-aided tracking”). In this case, the classification feature information may be used to more effectively form tracks. Feature information may be used to aid in track management and/or data association. Likelihood ratios may be formed on the classification feature information, and incorporated into track scores, which can be used as the basis for track initiation and termination. The feature information may be used to improve data association decisions. The feature likelihood ratio may be incorporated into the weighting of probabilistic data association (PDA) methods [4]. It may also be incorporated into track scores and thereby improve decisions among multiple track hypotheses (as in multi-frame assignment and MHT approaches) [5]. If there is a sufficient ability to predict the feature/attribute values, then the tracker state may be augmented to include the feature information [4, 6]. These methods assume that the feature statistics and their distributions (for target and non-target cases) are known well enough to be used in making tracking decisions. If this knowledge is not precise enough, it is possible that tracking performance could be degraded rather than enhanced.

Report Documentation Page

Form Approved
OMB No. 0704-0188

Public reporting burden for the collection of information is estimated to average 1 hour per response, including the time for reviewing instructions, searching existing data sources, gathering and maintaining the data needed, and completing and reviewing the collection of information. Send comments regarding this burden estimate or any other aspect of this collection of information, including suggestions for reducing this burden, to Washington Headquarters Services, Directorate for Information Operations and Reports, 1215 Jefferson Davis Highway, Suite 1204, Arlington VA 22202-4302. Respondents should be aware that notwithstanding any other provision of law, no person shall be subject to a penalty for failing to comply with a collection of information if it does not display a currently valid OMB control number.

1. REPORT DATE JUL 2011		2. REPORT TYPE		3. DATES COVERED 00-00-2011 to 00-00-2011	
4. TITLE AND SUBTITLE SPECSweb Post-Tracking Classification Method				5a. CONTRACT NUMBER	
				5b. GRANT NUMBER	
				5c. PROGRAM ELEMENT NUMBER	
6. AUTHOR(S)				5d. PROJECT NUMBER	
				5e. TASK NUMBER	
				5f. WORK UNIT NUMBER	
7. PERFORMING ORGANIZATION NAME(S) AND ADDRESS(ES) SPAWAR Systems Center Pacific (SSC-Pac), San Diego, CA, 92152-5001				8. PERFORMING ORGANIZATION REPORT NUMBER	
9. SPONSORING/MONITORING AGENCY NAME(S) AND ADDRESS(ES)				10. SPONSOR/MONITOR'S ACRONYM(S)	
				11. SPONSOR/MONITOR'S REPORT NUMBER(S)	
12. DISTRIBUTION/AVAILABILITY STATEMENT Approved for public release; distribution unlimited					
13. SUPPLEMENTARY NOTES Presented at the 14th International Conference on Information Fusion held in Chicago, IL on 5-8 July 2011. Sponsored in part by Office of Naval Research and U.S. Army Research Laboratory.					
14. ABSTRACT The Specular-Cued Surveillance Web (SPECSweb) multistatic tracker effectively reduces false track rate through the use of two amplitude thresholds. A high threshold is used to identify the occurrence of high-strength specular detection cues for track initiation. A low threshold is used for selective extraction of additional detections for track extension forward and backward in time. This approach significantly reduces the node-to-fusion-center communication loading requirements as well as reducing the output false track rate. At the time of the specular-cued track initiation, a historical (back)-track is reconstructed and output. In some cases, there may still be false tracks at the tracker output. We demonstrate a post-tracking classification method which identifies and removes any residual false tracks. Classification feature information for track-associated contacts is passed through the tracker and is available at its output. Discriminating true target tracks from false ones at the tracker output is made using a sequential probability ratio test (SPRT) based on feature information and kinematic track-quality. The method is shown to be effective in reducing false tracks when applied to a simulated data set.					
15. SUBJECT TERMS					
16. SECURITY CLASSIFICATION OF:			17. LIMITATION OF ABSTRACT Same as Report (SAR)	18. NUMBER OF PAGES 8	19a. NAME OF RESPONSIBLE PERSON
a. REPORT unclassified	b. ABSTRACT unclassified	c. THIS PAGE unclassified			

A final approach to using feature information with tracking (and the one pursued in this paper), is to apply the classification method only after the tracking process has been applied. This allows the kinematic association and filtering to proceed without the influence of feature information, but then filters the output based on the feature information. This is particularly relevant to the SPECSweb tracking approach, where the initiation scheme already significantly reduces the number of false tracks formed. Also, it provides a backtrack history of any of the target tracks that it outputs. The availability of additional contact features available in the historical backtracks provides larger, more effective statistical sample set for making certain classification decisions than those being made scan-by-scan. Residual false tracks which have been identified may either be terminated and/or suppressed from the operator's tracker output display. This approach will also be compatible with multi-sensor classification approaches which exploit class features that depend on the tracker's target state estimate. Future work will pursue this extension.

Section 2 in this paper describes the SPECSweb fusion/tracking algorithm. Section 3 describes the SPECSweb post-tracking classification method. Section 4 shows the classification method results on a simulated data set. Section 5 provides conclusions.

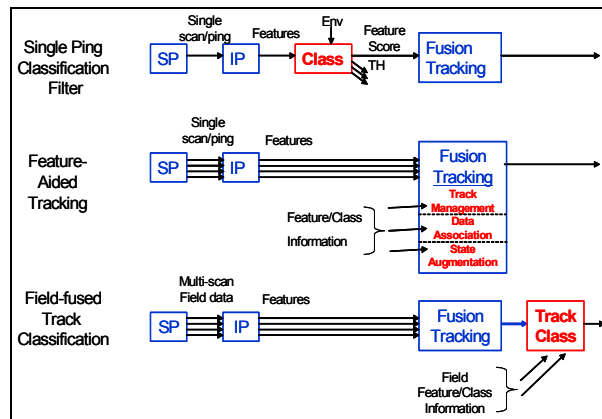


Figure 1. Approaches to tracking and classification (SP- signal processing; IP- information processing).

2 SPECSweb Algorithm Description

Detailed descriptions of the SPECSweb multistatic tracking algorithm and specular cueing approach are found in [2-3]. A brief description of the algorithm is included here. In the SPECSweb concept, it is envisioned that all single-sensor processing will be embedded on the receiver nodes, and store all the local output data. Each receiver collects the contacts corresponding to one source transmission as a single scan of “ping” data. Each sonar node (bistatic receiver processing a unique source-waveform) self-searches each processed (and locally stored) scan for contacts which exceed a high SNR threshold setting (HTH). The HTH

identifies very strong echoes, which likely correspond to targets that are in the “specular condition”. When in the specular geometry, there is greatly increased target strength, producing increased echo energy, as indicated by various models [7-8] and data analyses. The HTH normally rejects most (or all) of the false alarm clutter echoes, which have a lower distribution of amplitudes than do specular target echoes (though not necessarily lower levels than non-specular target echoes).

Contacts which cross the HTH are assumed to be “specular cues”, and (only) these are initially sent over the communication link to the multistatic fusion center for potential track initiation. There may be some increased track reporting latency using this approach. Evaluation metrics for studying the occurrence statistics of specular detection in multistatic fields have been developed [9].

Once a specular cue arrives at the fusion center, tentative reverse-time tracks are initiated. A cue is mapped to an x-y position in Cartesian coordinates, and this position with its associated error covariance are then sent as a snippet request to other nodes. These nodes calculate the appropriate snippet boundary in their respective measurement spaces within which data association would be possible, according to a specified gating parameter. Any contacts found within the snippet gate, and above the standard low-threshold (LTH), are then sent over the communication link for further processing. As track estimates are obtained, they themselves are used as the cues for selective data retrieval on prior scans stored on any of the nodes. The retrospective tracking (backtracks) continue until they meet a track termination criterion. Recovering track history in this fashion provides valuable contextual and track classification information.

The contacts belonging to the selected backtrack are then re-filtered in the forward-time direction, until the current time (of the initiating specular cue) is reached. At this point the track classification method may be applied on the retrospective historical track data. Tracking and classification updates continue in the forward-time direction updating with measurements found within the retrieval snippets of future scans.

SPECSweb uses logic-based track management (M of N initiation and K missed detections for termination). The tracker is implemented as an extended Kalman filter (EKF) with nearest neighbor data association and a nearly constant velocity (NCV) motion model.

3 Post-Tracking Classification

At the time of the specular initiation cue, a retrospective backtrack may be available. The classification information within backtracks are sequentially processed in a scan/time-ordered fashion. The process continues as forward-time tracking results are newly generated. Classification status is computed along the entire time duration of each track. Classification decisions may be used to suppress false tracks from the

operator display (while continuing to track them), or to terminate them.

3.1 Sequential Probability Ratio Test

The basis for the post-tracking classification decision is provided by the sequential probability ratio test (SPRT) [10]. We consider the two hypotheses, one for target and the other for non-target, as:

$$\begin{aligned} H_0 : & \Rightarrow \text{non - target} \\ H_1 : & \Rightarrow \text{target} \end{aligned} \quad (1)$$

The SPRT is given as the cumulative sum of the log of a number (J) of independent likelihood ratios formed from the data representing the features under consideration for classification. At the n^{th} update the SPRT is given by

$$L(n) = \sum_{i=1}^n \ln \left(\frac{P(D_{1,i}|H_1)}{P(D_{1,i}|H_0)} \cdot \frac{P(D_{2,i}|H_1)}{P(D_{2,i}|H_0)} \cdot \dots \cdot \frac{P(D_{J,i}|H_1)}{P(D_{J,i}|H_0)} \right) \quad (2)$$

The various D 's are measurable quantities from the data. We may then establish two thresholds:

$$A = \ln \left(\frac{1-\beta}{\alpha} \right); \quad B = \ln \left(\frac{\beta}{1-\alpha} \right) \quad (3)$$

where α is the false alarm probability (type I error) and β is the true target dismissal probability (type II error), and are parameters specified by the user. In our application, the SPRT is continuously updated until an *initial* classification is indicated by a threshold crossing as:

$$\begin{aligned} \text{Continue testing (pending)} & \Rightarrow \text{if } B \leq L(n) \leq A \\ \text{Accept } H_1 : & \Rightarrow \text{if } L(n) \geq A \\ \text{Accept } H_0 : & \Rightarrow \text{if } L(n) \leq B \end{aligned} \quad (4)$$

We also wish to consider the possibility that some tracks may change status, i.e., change from being a true target track to becoming a false track, or vice versa. This can occur in tracking targets amongst dense clutter, where a true track starts associating nearby false contacts and then progressively “wanders” off. In order to accommodate this possibility we have chosen to implement adjustable thresholds after the initial target/non-target determination has been made. This is done by resetting the thresholds by raising/lowering them according to the new maximal/minimal values of L . The following adjustment and testing scheme is used:

$$\begin{aligned} & \text{if } H_1 \text{ and } L(k) > A(k) \\ & \quad \Rightarrow \text{maintain } H_1 \\ & \quad \Rightarrow \text{set } A(k+1) = L(k) \\ & \quad \Rightarrow \text{set } B(k+1) = L(k) - \Delta \\ & \text{else if } H_1 \text{ and } L(k) < B(k) \\ & \quad \Rightarrow \text{change to } H_0 \\ & \quad \Rightarrow \text{set } A(k+1) = L(k) + \Delta \\ & \quad \Rightarrow \text{set } B(k+1) = L(k) \\ & \text{else if } H_0 \text{ and } L(k) > A(k) \\ & \quad \Rightarrow \text{change to } H_1 \\ & \quad \Rightarrow \text{set } A(k+1) = L(k) \\ & \quad \Rightarrow \text{set } B(k+1) = L(k) - \Delta \\ & \text{else if } H_0 \text{ and } L(k) < B(k) \\ & \quad \Rightarrow \text{maintain } H_0 \\ & \quad \Rightarrow \text{set } A(k+1) = L(k) + \Delta \\ & \quad \Rightarrow \text{set } B(k+1) = L(k) \end{aligned} \quad (5)$$

end if

where k indicates the current update and Δ is the difference of the thresholds, i.e.,

$$\Delta = A(1) - B(1). \quad (6)$$

where $A(1)$ and $B(1)$ are set to A and B in Eq. (3).

Figure 2 shows a comparison of an example SPRT output corresponding to a track (#28 of section 4), which changes state as: false (negative slope) \rightarrow true (positive slope) \rightarrow false (negative slope). The track is initiated by a specular cue around which it is a true track. Further backward and forward in time the track updates are provided by false contacts and the track becomes false. The adjustable threshold method makes an earlier and better classification of the target section than the fixed method (scans 2301-3250 vs. scan 2900-3250).

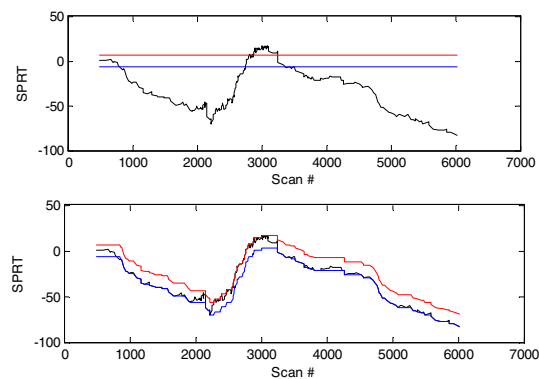


Figure 2. SPRT (black) with fixed thresholds (top) and adjustable thresholds (bottom); target threshold (red), non-target threshold (blue).

3.2 Kinematic Track Quality

Many tracking algorithms utilize an SPRT for track initiation which includes both a kinematic and a signal-

related contribution [11]. Here we use only the kinematic portion of this approach, and it will be applied to the tracker output rather than the tracker input. The signal-related contribution depends on a priori knowledge of P_D and P_{FA} , which in practice may be difficult to know well enough. While P_{FA} may be ascertained by analysis of in-situ data, P_D for multistatic systems is complex to estimate, being dependent on a complex space/time evolving acoustic environment, as well as the source-receiver positions, target aspect angle, etc. These dependencies may be estimated using sophisticated sonar equation models; however they are often still not of sufficient fidelity to adequately predict precise performance. An approach to estimating P_D from the arriving data has been proposed [12]. Nevertheless, given the difficulties of predicting P_D , we choose to focus on only the kinematic contribution in this work.

The assumption for the kinematic likelihood ratio is that target-originated contacts will be distributed according to Gaussian statistics with the mean at the state estimate, whereas false alarm contacts are assumed to be uniformly distributed over the association gate. The likelihood ratio for the kinematic portion of the SPRT is given by [11]

$$LR_K = \frac{V_G \cdot e^{(-d^2/2)}}{(2\pi)^{M/2} \sqrt{|S|}} \quad (7)$$

where the volume of the ellipsoidal association gate is given by

$$V_G = \frac{\pi^{M/2} \cdot G^{M/2} \cdot \sqrt{|S|}}{\Gamma\left(\frac{M}{2} + 1\right)} \quad (8)$$

Γ is the gamma function, M is the dimensionality of the measurement and G is the value corresponding to a gate of a specified association probability (depends also on M). S is the Kalman residual covariance matrix, given by $S = HPH^T + R$, where H is the linearized measurement (Jacobian) matrix, R is the measurement covariance matrix, and P is the predicted state covariance matrix. d^2 is the norm of the residual vector given by

$$d^2 = [y(k) - h(\hat{x}(k|k-1))]^T S^{-1} [y(k) - h(\hat{x}(k|k-1))] \quad (9)$$

where y is the measurement data, $\hat{x}(k|k-1)$ is the projected target state, and h is the non-linear measurement function. Simplifying (5) yields

$$LR_K = \frac{e^{(-d^2/2)} \cdot (G/2)^{M/2}}{\Gamma((M/2) + 1)} \quad (10)$$

The calculations to obtain d^2 are made during iterations of the Kalman filter update, and are saved and output along with the tracker's updated target state estimates. The likelihood ratios are formed and the SPRT is calculated at each iteration of the Kalman update, except

when there is no contact associated with the track update (i.e., a track "coast" condition).

3.3 Classification Feature Score

We assume that per-contact classification feature scores have been computed in the processing upstream of the tracker. These may be, for example echo SNR-based or related echo energy size/shape. Here, we don't address any specific or particular feature, but consider the case of a "generic" feature, for which a score is computable. When a contact is assigned to a track update, information about that contact, including the feature score is saved and output along with the updated state estimate.

We assume that we have some knowledge of the underlying target and non-target distributions for the generic feature score that is computed. If these distributions are not known, target and non-target training data may be used to obtain estimates of their probability density functions using kernel density estimation methods. Given the target/non-target distributions, and the feature score, we can form the likelihood ratio for the feature as

$$LR_F = \frac{p(D_F|H_1)}{p(D_F|H_0)} \quad (11)$$

which is a ratio of the corresponding probability densities, given the value of the feature score D_F .

The likelihood calculations are made after each update of the Kalman filter if a contact updates the track estimate. If the track is in a "coast" condition, then the likelihood ratio is not formed because there is no associated feature information. The SPRT is updated sequentially as new data becomes available.

3.4 Combined Classification

The post-track classification may utilize both of the likelihood ratios (kinematic and feature) just described. In this case the SPRT becomes:

$$L(n) = \sum_{i=1}^n \ln[LR_K(i) \cdot LR_F(i)] \quad (12)$$

4 Classification Results

Multistatic data was simulated using the Passive-Active Contact Simulation Tool (PACsim) [13]. Figure 3 shows the scenario, with 5 fixed sources (red) and 16 fixed receivers (green) distributed over a surveillance area. Pings are emitted every minute, cycling amongst the sources, and alternating between FM and CW waveforms. The scenario lasts about 6.8 hours, with 409 pings and 6,541 measurement scans (16 scans per ping). Eight targets are simulated as described in Table 1 and as depicted in figure 3.

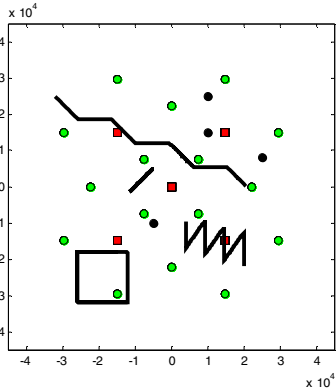


Figure 3. Simulation Scenario (distances in 10 km); sources (red), receivers (green), targets (black).

Table 1. Simulated Targets

#	Description
1	6 course changes of $\pm 45^\circ$; (loose zig-zag), 5 kts
2	Fixed target to the north
3	6 course changes of 180° ; back and forth, 5 kts
4	Fixed target to the south
5	6 course changes of 90° ; (box), 7.5 kts
6	Fixed target
7	6 course changes of 135° ; (tight zig-zag), 5 kts
8	Fixed target to the east

The target SNRs are computed by solving the sonar equation for each source-receive-target-waveform combination in a representative acoustic environment with generic airborne multistatic system components. The simulation includes modeling of transmission loss, reverberation, aspect-dependent target strength, noise background, and system gains. Measurements of contact time delay (τ), bearing (θ), and Doppler (ν) were simulated using assumed errors of $\sigma_\tau=0.1$ sec (FM), $\sigma_\tau=0.4$ sec (CW), $\sigma_\theta=4^\circ$ and $\sigma_\nu=0.4$ m/s. Non-target (clutter) contacts were distributed uniformly in measurement space and with SNRs following an exponential distribution above the detection threshold. The number of false contacts per scan is Poisson distributed ($\lambda=30$) per scan. A generic classification feature score was simulated for each contact with random draws from the following normal distributions:

- Non-Target: $N(\mu_c = 0, \sigma_c = 10)$
- Target (case1): $N(\mu_{T1} = 6, \sigma_i = 10)$
- Target (case 2): $N(\mu_{T2} = 10, \sigma_i = 10)$

Figure 4 shows a plot of these distributions and their associated ROC curves vs. the chance line (indicated in green). We see that target case 2 has more separation from the clutter distribution than case 1, and therefore, greater classification potential. Figure 5 shows the cumulative output of the SPECSweb tracker with a good choice of parameter settings. We see that the result for this case is excellent: good tracking with no false tracks. The average input and output P_D were 0.3 and 0.9, respectively. The target tracks average purity (target-to-

total contact updates) was 91% and the percentage of “coasts” (scans without a contact update) was 92%. For this scenario, performance is so good that it does not require post-track classification.

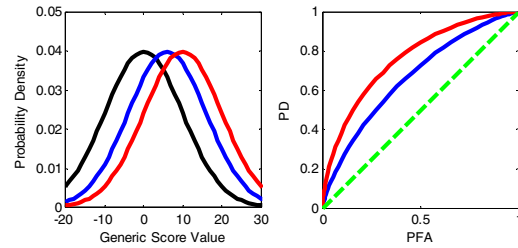


Figure 4. Generic classification feature score (Target case1-blue, Target case2-red, Clutter-black); distributions (left), ROC Curves (right).

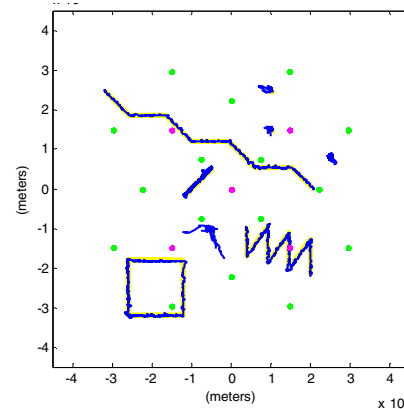


Figure 5. Optimized SPECSweb tracking output without classification; target true trajectories (yellow), tracks (blue), sources (red), receivers (green).

Unlike the performance just seen, more challenging scenarios and acoustic environments may yield a number of false output tracks, even with the SPECSweb algorithm. In order to create such a test data set for our classification analysis, we now select sub-optimum tracking parameters to induce an increase in the false track rate. This was done by changing the track management logic to make it easier to initiate and harder to terminate tracks ($M/N/K = 6/16/50$ vs. $M/N/K = 6/81/150$). Figure 6 shows the resulting tracker performance. We see a cluttered output display, composed of 65 tracks, some of them extending beyond the surveillance box boundary. This test data will serve as a baseline case (without classification) and as the input to the post-tracker classifier. Some tracks are true target tracks; others are initiated by true target contacts and continue on (wandering) with false alarms, or, they are wholly and completely false tracks. The mapping of targets to output track number is given as: TGT1 (10), TGT2 (2,58), TGT3 (4,7), TGT4, (1,31,59,64), TGT5 (3), TGT6 (8,28,38), TGT7 (5), TGT8 (11,39).

The classification method is now applied to the tracker output (of figure 6). The first case we consider is to use

only the kinematic information, as described in section 3.2, with decision thresholds set corresponding to $\alpha=\beta=0.001$. Figure 7 shows the entire time-extent of each of the 65 input tracks (referenced by scan index), from the earliest point of the backtrack to the last update of the forward track termination. The time of the track-initiating specular cue is shown overlaid by the magenta marker. The tracks are color-coded by the classification status obtained: target (red), non-target (green), and decision pending more information (blue). We observe that many of the tracks are classified as false, and that the classification decisions are usually made prior to the occurrences of the specular cues (tracker's initial output). Most of the target tracks are detected early and have continuous hold, except in a few instances when the classification status changes from true-to-false (or vice versa). This is due to tracks which "wander", being fed by false alarms and which most often occur for the fixed (non-mobile) targets. The true (red) and pending (blue) tracks are shown plotted in figure 8, where we see good correspondence between the true tracks and the eight known target trajectories, and a significant reduction in the false (clutter) tracks observed. The classifier in this case (figure 8) shows good performance compared to the input case (figure 6).

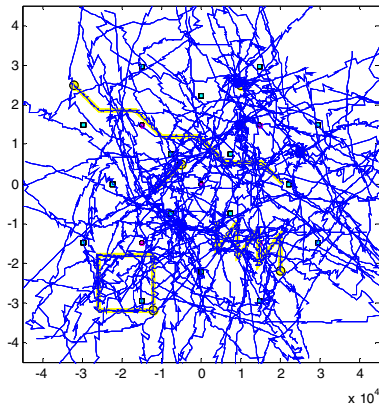


Figure 6. Data set with induced false tracks for classification evaluation; 65 output tracks (blue), target true trajectories (yellow).

Next we show examples only using the generic feature information, as described in section 3.3, with decision thresholds nominally set corresponding to $\alpha=\beta=0.001$. Figure 9 shows the output of the classifier for Case 1 (heavily overlapping target/non-target distributions). Here it is observed that classification decisions take a longer time to be reached, as indicated by the increases in the amount of pending status (blue). Although the classification decisions for targets are quite good, many of the false tracks are not classified prior to the specular cue initiation. Figure 10 shows the track display for this case, which shows good tracking on the targets, but with a few falsely classified true-tracks appearing. There is a large

number of pending tracks shown which confuse the output. One could choose to display only confirmed true target tracks, if desired, which change the impression significantly. Nonetheless, the results are still much better than the input case (figure 6).

Figure 11 shows the effect of relaxing the false alarm and false dismissal parameters (changing $\alpha=\beta=0.001$ to $\alpha=\beta=0.01$). Classification decisions are reached much faster (fewer observable pending tracks), as expected, though perhaps with worsening false track rate.

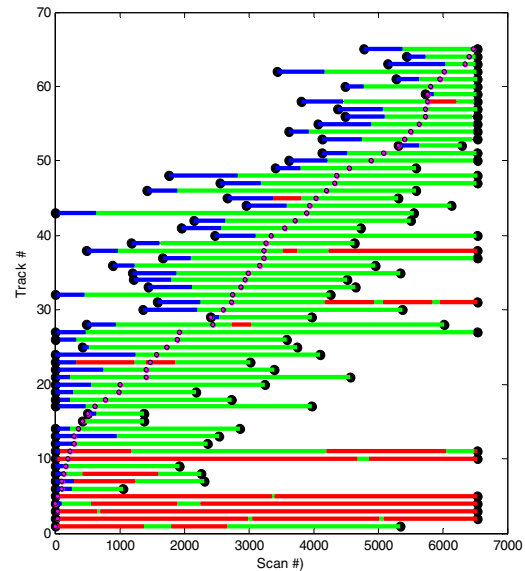


Figure 7. Classification vs. track, for kinematic information only; pending (blue), non-target (green), target (red); specular track initiation (magenta).

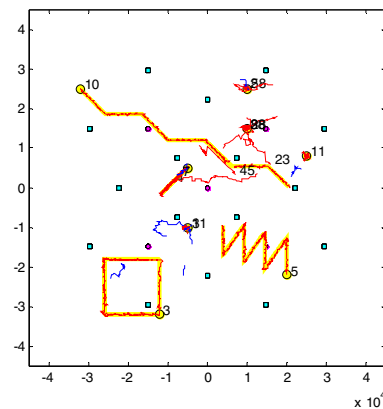


Figure 8. Output for kinematic information only; target trajectories (yellow), classified target (red); pending classification (blue).

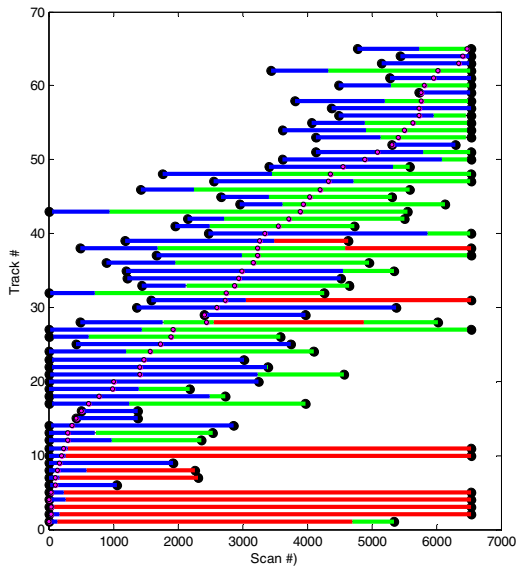


Figure 9. Classification vs. track, for feature information only (case 1); colors as in figure 7.

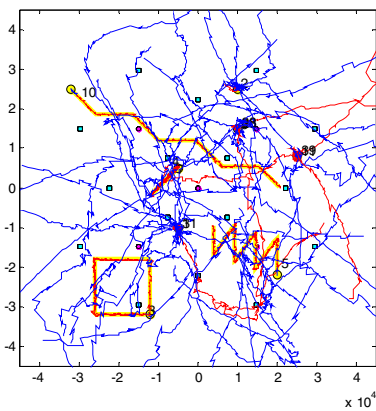


Figure 10. Classification results for feature information only, case 1, $\alpha=\beta=0.001$.

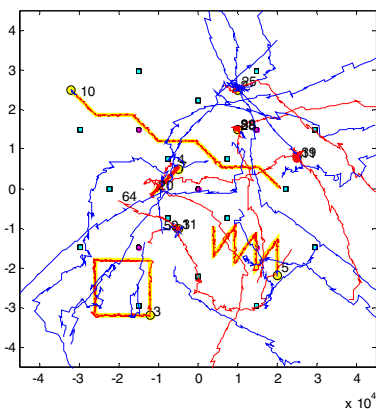


Figure 11. Output for feature information only, case 1, $\alpha=\beta=0.01$.

Figures 12 and 13 correspond to the Case 2, where the feature score is more separable (and with original settings of $\alpha=\beta=0.001$). Here we obtain even better performance, though it is not as good as the results obtained with kinematic information only. Here, the total percentage of pending track-time (of total track-time) is reduced to 17% from 42% (see in figures 9).

Next we consider the effect of combining the kinematic and feature, as described in section 3.4, with decision thresholds again corresponding to $\alpha=\beta=0.001$. The results are shown in figures 14. In this case we obtain the best results, with the cleanest, de-cluttered output display. All eight targets are tracked well. When true tracks wander away from real targets, they are classified false and suppressed. Classification decisions are made earlier, and changes in state are more robust to the truth. This example shows the power of combining all available information into the classifier likelihood ratio formulation.

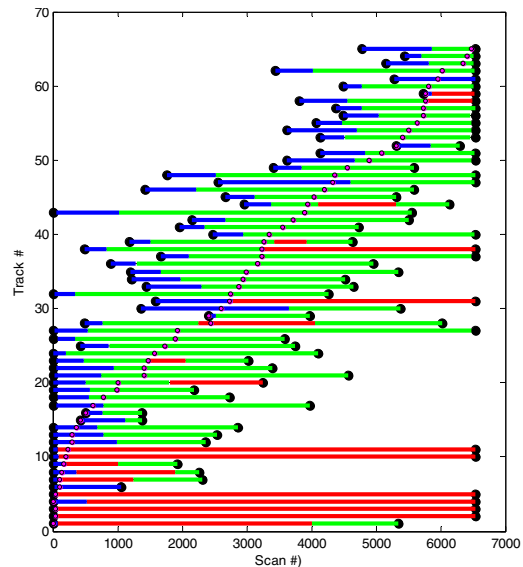


Figure 12. Classification vs. track, for feature information only (case 2); colors as in figure 7.

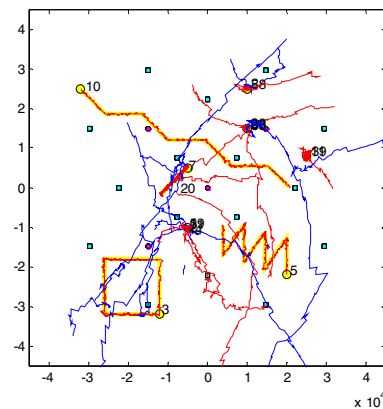


Figure 13. Output for feature information only, case 2, $\alpha=\beta=0.001$.

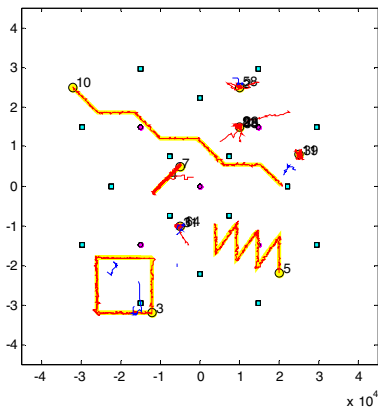


Figure 14. Output for combined kinematic and feature information, case 2, $\alpha=\beta=0.001$.

5 Conclusions

A post-tracking classifier method compatible with SPECSweb has been described, and has been shown to be effective in reducing false tracks in the output. So far, the formulation includes kinematic track-quality measures and per-contact feature scores. Their likelihood ratios have been used in an adjusting sequential probability ratio test to arrive at classification decisions. Often, these decisions are made during the backtrack section of the total track (before the specular cue) and the non-target and/or pending tracks. Table 2 summarizes the performance of the cases evaluated. Future work will investigate the incorporation of specific target-aspect (and therefore tracker output state estimate) dependent field features.

Table 2. Output class percentages

#	% <i>True</i>	% <i>False</i>	% <i>Pend</i>
Kinematic	21	66	13
Feature (case 1)	25	33	42
Feature (case 2)	27	56	17
Both (case 1)	22	66	11
Both (case 2)	23	67	9

References

- [1] D. Grimmer, An Effective Approach to Multistatic Tracking in Dense Clutter Environments, Proceedings of the International Symposium on Underwater Reverberation and Clutter, NATO Undersea Research Centre, La Spezia, Italy, September 2008.
- [2] D. Grimmer, Multistatic Target Tracking using Specular Cue Initiation and Directed Data Retrieval, in Proceedings of the 11th International Conference on Information Fusion, July 2008, Cologne, Germany.
- [3] D. Grimmer, Specular-Cued Multistatic Sonar Tracking on the SEABAR'07 Dataset, in Proceedings of the 12th International Conference on Information Fusion, July 2009, Seattle, Washington, U.S.A.
- [4] E. Hanusa, W. H. Mortensen, D. Krout, J. McLaughlin, Improving Target Tracking Performance by Incorporating Classification Information, in Proceedings of the 12th International Conference on Information Fusion, July 2009, Seattle, Washington, U.S.A.
- [5] Y. Bar-Shalom, T. Kirubarajan, C. Gokberk, Tracking with classification-aided multiframe data association, IEEE Transactions on Aerospace and Electronic Systems, Vol. 41, Issue 3, July 2005.
- [6] X. Wang, B. La Scala, R. Ellen, Feature-Aided Probabilistic Data Association for Multi-Target Tracking, in proceedings of the 11th International Conference on Information Fusion, July, 2008, Cologne, Germany.
- [7] R. P. Hodges, Underwater Acoustics: Analysis, Design and Performance of Sonar, John Wiley and Sons, Chichester, U.K., 2010.
- [8] R. F. Gragg, The BASIS-3D Acoustic Target Strength Model, NRL/FR/7140--07-101052, Washington D.C., U.S.A., Naval Research Laboratory, 2002.
- [9] D. Grimmer, S. Sullivan, Sr., and J. Alsup, Modeling Specular Occurrence in Distributed Multistatic Fields, in Proceedings of the IEEE OCEANS'08 Conference, July 2008, Kobe, Japan.
- [10] A. Wald, Sequential Analysis, New York: Dover Publications, 1973.
- [11] S. Blackman and R. Popoli, Design and Analysis of Modern Tracking Systems, Norwood, MA: Artech House, 1999, ch. 6.3.
- [12] K. Jamieson, M. Gupta, D. Krout, Sequential Bayesian Estimation of the Probability of Detection for Tracking, in proceedings of the 12th International Conference on Information Fusion, July, 2009, Seattle, WA, USA.
- [13] D. Grimmer, C. Wakayama, R. Ricks, Simulation of Passive and Multistatic Active Sonar Contacts, to appear in Proceedings of the 4th International Conference on Underwater Acoustic Measurements: Technologies and Results, June, 2011, Kos, Greece.